Am J Transl Res 2016;8(11):4694-4704
www.ajtr.org /ISSN:1943-8141/AJTR0036120

Original Article

T3 inhibits the calcification of vascular smooth muscle cells and the potential mechanism

Xiaodan Chang[1,2*], Baohong Zhang[3*], Li Lihua[4], Zhichun Feng[1]

[1]Department of Neonatology, Affiliated Bayi Children's Hospital, Clinical Medical College in PLA Army General Hospital, Southern Medical University, Beijing 100007, China; [2]Department of Neonatology, The Second Central Hospital of Baoding City, Baoding 072750, China; [3]Department of Pediatrics, The Hospital of Tsinghua University, Beijing 100084, China; [4]Department of Pediatrics, Beijing Luhe Hospital Affiliated to Capital Medical University, Beijing 101149, China. [*]Equal contributors.

Received July 18, 2016; Accepted November 2, 2016; Epub November 15, 2016; Published November 30, 2016

Abstract: Objective: This study aimed to investigate the potential molecular mechanism underlying the T3 induced vascular calcification and phenotype transformation of vascular smooth muscle cells (VSMCs). Methods: Rat thoracic aortic smooth muscle cells (A7r5) were cultured in vitro and randomly assigned into normal control group, calcification group, T3 group and inhibitor group. Results: When compared with normal control group, the osteocalcin content, ALP activity, Osterix and Runx2 mRNA expression and OPN protein expression increased significantly ($P<0.01$), and the protein expression of SMα and SM22α reduced dramatically in A7r5 cells of calcification group ($P<0.01$). After T3 treatment, the osteocalcin content and ALP activity reduced markedly, mRNA expression of Osterix and Runx2 and OPN protein expression reduced significantly. However, MMI (inhibitor of T3) was able to block the above effects of T3. When compared with calcification group, Osterix and Runx2 mRNA expression and OPN protein expression increased markedly ($P<0.01$). In addition, the protein expression of ERK1/2, p-ERK, Akt and p-Akt increased significantly in calcification group. In the presence of integrin αvβ3/ERK blocker (PD98059) and/or PI3K/Akt antagonist (LY294002), T3 was still able to inhibit the calcification, and this effect was similar to that after treatment with inhibitors alone. Moreover, LY294002 had a better inhibitory effect as compared to PD98059. Conclusion: T3 may act on PI3K/Akt signaling pathway to inhibit the phenotype transformation of VSMC, which then suppresses the calcium/phosphate induced calcification of rat VSMCs. Thus, T3 is an endogenous molecule that can protect the blood vessels against calcification.

Keywords: Thyroid hormone, vascular calcification, vascular smooth muscle cells, phenotype switch, signaling pathway

Introduction

Thyroid hormones (THs) include 3,5,3'-triiodothyronine (T3) and thyroxine (T4). T3 is a major active form of THs and may act directly on the myocardium, vascular smooth muscle cells (VSMC) and endothelial cells. It may bind to the specific receptor to directly or indirectly induce biological effects on the cardiovascular system [1]. In critically ill neonates, especially preterm infants, the hypothalamus is immature, which together with other factors (such as infection, stress and metabolic disorder) may increase the secretion of catecholamines and glucocorticoids and inhibit 5'-deiodinase activity. Thus, the conversion of T4 into T3 is inhibited, leading to the reduction in T3. Under this condition, there are no symptoms of thyroid dysfunction [2, 3]. This process may be accompanied by vascular calcification in neonates and cause pulmonary hypertension, which then affect lung function, leading to severe complications such as heart failure and bronchopulmonary dysplasia.

In recent years, studies revealed that vascular calcification is a reversible and active process regulated by multiple factors [4] and has involved some cytokines and signaling pathways. Our previous study showed vascular smooth muscle cells (VSMCs) in the arterial media, major participants in vascular calcification, lost their original phenotype and acquired osteogenic phenotype accompanied by reduction in muscle fibers and cytoskeletal proteins and increased secretion of extracellular matrix, leading to vascular remodeling characterized by thickening of blood vessel wall and lumen ste-

nosis [5, 6]. The phenotype transformation of VSMCs is regulated by several signaling pathways including MAPK pathway, PI3K pathway and CAMP pathway. In addition, the biologically active factors such as adrenomedullin, C-type natriuretic peptide, angiotensin and aldosterone in vascular tissues are also involved in the regulation of vascular calcification [7-9]. Thus, to investigate the signaling pathways related to the phenotype transformation of VSMCs may provide evidence for reversal of vascular calcification.

Previous study [10] has confirmed that T3 content reduces in the plasma of rats with calcification and calcium deposits in the blood vessels. At 10 days after T3 treatment (0.2 mg/kg), the calcium deposition and alkaline phosphatase activity of the blood vessels reduce, the reduced expression of SM22α and SMα (two markers of smooth muscle cells) restores, expression of osteogenesis related OPN is down-regulated, and the expression of Runx2 and Osterix (two important transcription factors for bone differentiation) also reduces. This study aimed to further investigate the molecular target and mechanism in the T3 induced inhibition of osteogenic phenotype switch of VSMCs, which may provide evidence for the fact that THs are important molecules able to inhibit the vascular calcification and the osteogenic phenotype switch of VSMCs.

Materials and methods

Cells and reagent

Rat thoracic aortic VSMCs (A7r5 cells) were purchased from the Cell Bank of Shanghai Institute of Biological Sciences of Chinese Academy of Science. Fetal bovine serum (FBS), high glucose DMEM, penicillin, streptomycin (Hyclone, USA), Alizarin red solution, β- Glycerol phosphate, calcium chloride ($CaCl_2$), 3,3',5'-Triiodo-L-thyronine, 2-(Methylthio)benzimidazole (Sigma, USA), antibodies against OPN and SM22α (Bioworld), antibodies against ERK1/2, p-ERK, Akt and p-Akt (Cell signaling), α-actin antibody (Boster), Alkaline Phosphatase (ALP) Detection Kit (Beyotime Biotechnology), rat osteocalcin (BGP) ELISA kit and other analytically pure reagents were used in the present study. Primers for RT-PCR were synthesized in Shanghai Jierui Biotech Co., Ltd. Cell incubator (HERACELL150i; Thermo scientific) and microplate reader (multiscan MK3; Thermo Fisher Scientific) were used for detection.

Cell culture

Cells were in a good growth status and spindle-shaped. Cells were maintained in 4 ml of DMEM containing 10% FBS and 1% streptomycin/penicillin at 37°C in an environment with 5% CO_2. Cells were passaged on the second day. When the cell confluence reached 100%, cells were digested with trypsin-EDTA (1 ml/25 cm^2, 2 ml/75 cm^2), and cell morphology was observed under a light microscope. Cells were passaged until the number of cells was enough for following experiments. Cells with good growth status were used in following experiments.

Grouping

Cells were seeded into 6-well plates at a density of 1×10^5 cells/L and maintained in DMEM containing 10% FBS. When the cell confluence reached 80%, cells were divided into following 7 groups: 1) Normal control group: cells were maintained in DMEM without other treatments. 2) Calcification group: Cells were treated with 5 mmol/L β-glycerophosphate and 2.5 mmol/L $CaCl_2$. 3) Calcification+T3 (10^{-7} mol/L) group: In the presence of calcium and phosphorus, cells were treated with T3 at different concentrations (10^{-7}, 10^{-8} and 10^{-9} mol/L). 4) Calcification+T3 (10^{-8} mol/L) group. 5) Calcification+T3 (10^{-9} mol/L) group. 6) MMI group: Cells were treatment with MMI at 10^{-6} mol/L. 7) Calcification+MMI group: In the presence of calcification induction, cells were treated with MMI at 10^{-6} mol/L.

Treatment of cells

The medium was refreshed once every 2 days. Cells were harvested at 3 h, 6 h, 12 h, 1 d, 3 d, 6 d and 12 d. The optimal concentration of T3 and optimal duration of T3 treatment were determined. Then, calcified cells were treated again with T3 at the optimal concentration for the optimal duration. Then, cells were harvested for the detection of ERK1/2, p-ERK, Akt and p-Akt protein expression by Western blot assay, aiming to elucidate the role of PI3K/Akt and αvβ3/ERK in T3 induced vascular calcification. In calcification+T3 group, Akt and ERK were found to be activated. Moreover, to investigate the signaling pathway involved in phenotypic

Table 1. Primers used for PCR of target genes

Gene	Sequences
Runx2	Forward 5'-GAT GCC TTA GTG CCC AAA TGT-3'
	Reverse 3'-GGC TGA AGG GTG AAG AAA GC-5'
Osterix	Forward 5'-CCC AAC TGT CAG GAG CTA GA-3'
	Reverse 3'-CCT CTT GCC ACA GAA AAG C-5'
β-actin	Forward 5'-AGG AAA TCG TGC GTG ACA T-3'
	Reverse 3'-GAA CCG CTC ATT GCC GAT AG-5'

transition of VSMCs, PI3K/Akt and αvβ3/ERK inhibitor LY294002 and PD98059 were administered respectively: Normal control group; Calcified cells +LY294002 (0, 15 and 30 μmol/L) group; Calcified cells+PD98059 (0, 20 and 40 μmol/L) group; Calcified cells + LY294002 (30 μmol/L) + T3 (6 h, 10^{-7} mol/L) group; Calcified cells + PD98059 (40 μmol/L) +T3 (6 h, 10^{-7} mol/L) group. Each experiment was performed at least three times with triplicate cultures used in every experiment unless stated otherwise.

Alizarin red staining

Alizarin red staining was used to assess Ca deposition in VSMC cell layers, by which Alizarin red S dye binds with Ca ions in cell layer matrix. Cells were seeded into 6-well plates. The medium was removed, and cells were washed in PBS twice. Then, cells were fixed in 4% neutral formalin (2 ml/well) for 30 min. After removal of formalin, cells were washed in PBS twice, followed by incubation with 0.1% Alizarin Red (1 ml/well) for 3-5 min. After washing PBS, cells were observed under a light microscope for calcified nodules. Three samples were selected from each group, and one field was randomly selected form each sample at ×100. The number of calcified nodules was compared between groups. The calcified nodules were orange.

Detection of osteocalcin content

Cells were seeded into 6-well plate. The medium was removed and cells were washed in PBS thrice. The content of osteocalcin (BGP) was measured with a commercially available kit by enzyme-linked immunosorbent assay (ELISA) according to manufacturer's instructions (Shanghai Meiyan Biotech Co., Ltd; Ek-R30432). Cells were lysed, and cell lysate was added to each well, followed by incubation. After addition of enzyme and washing, visualization was done, which was then stoped by addition of stop solution. The optical density (OD) was measured at 450 nm within 15 min.

Detection of ALP activity

Cells were seeded into 6-well plates. The medium was removed and cells were washed thrice with PBS. The ALP activity was measured according to manufacturer's instructions with a kit (P0321; Beyotime Biotech Co., Ltd). In brief, 300 μl of 0.1% Triton X-100 was added to each well, followed by incubation at 4°C for 12-24 h. The lysed cells were pipetted and then transferred into a centrifuge tube, followed by centrifugation. In standard sample wells, standard sample was added at 4, 8, 16, 24, 32 or 40 μl; in sample wells, samples were added at 50 μl. Incubation was done at 37°C. The hydrolysis of para-nitrophenyl phosphate as a chromogenic substrate within 1 min may produce 1 μmol p-nitrophenol, which requires 1 unit of ALP activity.

RT-PCR

Cells were harvested and total RNA was extracted with Trizol reagents. The residual DNA in RNA was removed by DNAse I. Synthesis of cDNA: 5 μl of total RNA was mixed with 1 μl of oligo(dT)18 primers (0.5 μg/μl), followed by centrifugation. After incubation at 70°C for 5 min, the mixture was incubated in water, followed by transient centrifugation. Then, 5 μl of 5× reaction buffer, 5 μl of 10 mmol/L dNTP, 1 μl of reverse transcriptase (200 U/μl) and 0.5 μl of RNase inhibitor (20 U/μl) were added, followed by centrifugation. The mixture was incubated at 37°C for 5 min, at 42°C for 1 h and then at 70°C for 10 min to stop the reaction. The mixture was allowed to cool on ice. PCR was performed with ABI PRISM® 7500 thermal cycler and the conditions were as follows: predenaturation at 95°C for 5 min, and a total of 35 cycles of denaturation at 95°C for 45 s, annealing at 58°C for 45 s and extension at 72°C for 50 s, followed by a final extension at 72°C for 10 min. The PCR products were subjected to agarose gel electrophoresis, and bands were scanned for the analysis of optical density. Experiment was done thrice, and GAPDH served as an internal control. The relatively mRNA expression of each gene was determined. The primers used for PCR are shown in **Table 1**.

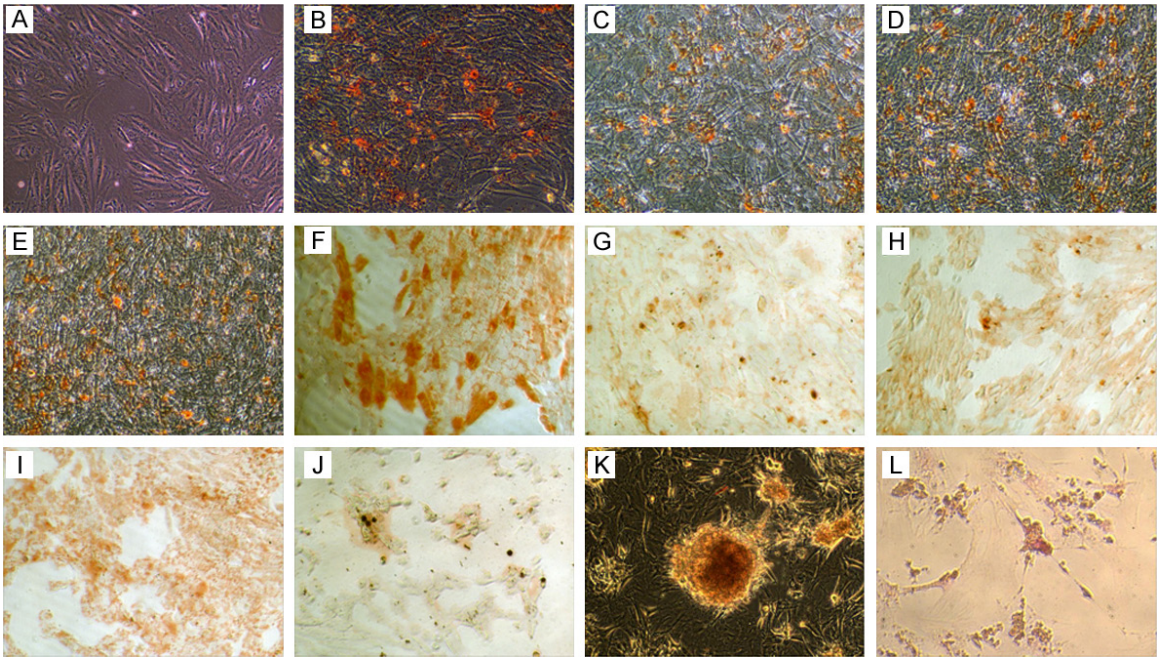

Figure 1. Calcified nodules in A7r5 cells after different treatments (Alizarin red S staining; ×100). A: Normal control group; B: Calcification group (12 d); C: Calcification + T3 group (10^{-7} mol/L, 3 h); D: Calcification + T3 (10^{-8} mol/L, 3 h); E: Calcification + T3 group (10^{-9} mol/L, 3 h); F: Calcification group; G: Calcification + T3 (10^{-7} mol/L, 6 h); H: Calcification + T3 (10^{-8} mol/L, 6 h); I: Calcification + T3 (10^{-9} mol/L, 6 h); J: Calcification + T3 (10^{-7} mol/L, 12 h); K: Calcification + T3 (10^{-7} mol/L, 1 d); L: Calcification + T3 (10^{-7} mol/L, 3 d).

Western blotting

Cells from each group were subjected to protein extraction with BCA method. Then, 40 μl of protein sample was mixed with equal volume of 2× loading buffer (50 mmol/L, PH6.8 Tris-Hcl, 2% SDS, 10% glycerin, 0.1% bromophenol blue and 1 mol/L DTT), followed by being boiled for 3 min. The mixture was subjected to 10% SDS-PAGE at 2 mA for 3 h. Then, the proteins were transferred onto PVDF at 20 V for 1.5 h. The membrane was blocked at room temperature for 4 h, and then incubated with primary antibody at 4°C over night. After washing in TBST thrice (15 min for each), the membrane was incubated with secondary antibody at room temperature for 2 h. Following washing in TBST thrice (15 min for each), visualization was performed with ECL, and bands were scanned with image gel analysis system. The optical density (OD) of each band was determined and then normalized to that of GAPDH as its relative protein expression. Experiment was performed three times.

Statistical analysis

Data are expressed as mean ± standard deviation (SD). Means were compared with t test between two groups and with one way analysis of variance (ANOVA) among groups followed by Student2Newman2Keuls test. A value of $P<0.05$ was considered statistically significant.

Results

Effect of T3 on calcium and phosphorus induced calcification of A7r5

After induction with β-glycerophosphate and CaCl2 for 12 days, Alizarin red S staining showed orange calcified nodules in calcification group; when compared with calcification group, the orange calcified nodules reduced significantly in T3 group, and the higher the T3 concentration, the smaller the number of orange calcified nodules was. In addition, cells were treated with T3 for 3 h, 6 h, 12 h, 1 d and 3 d, but the calcified cells had a low adherence. Thus, after induction for 3 days, a majority of cells was suspended in the medium. On the basis of osteocalcin content and ALP activity, the optimal concentration of T3 was 10^{-7} mol/L and the optimal duration of T3 treatment was 6 h. Thus, in following experiments, cells were treated with 10^{-7} mol/L T3 for 6 h (**Figure 1**).

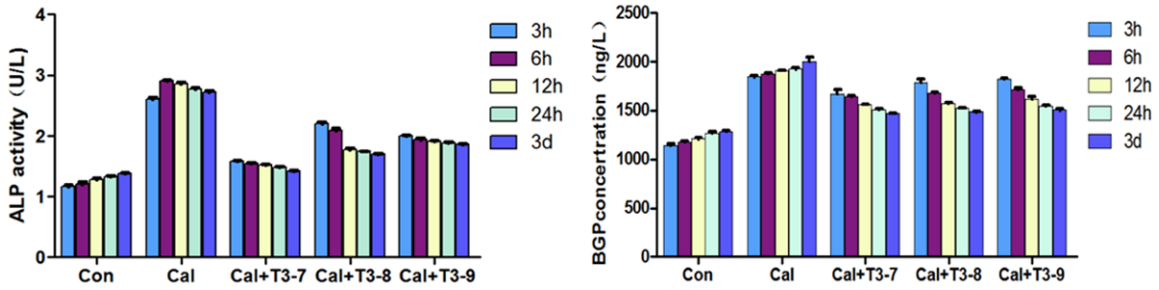

Figure 2. BGP content and ALP activity of A7r5 cells after different treatments. Con: normal control; Cal: calcification group; Cal + T3-7: calcification + T3 (10^{-7} mol/L); Cal + T3-8: calcification +T3 (10^{-8} mol/L); Cal + T3-9: calcification +T3 (10^{-9} mol/L).

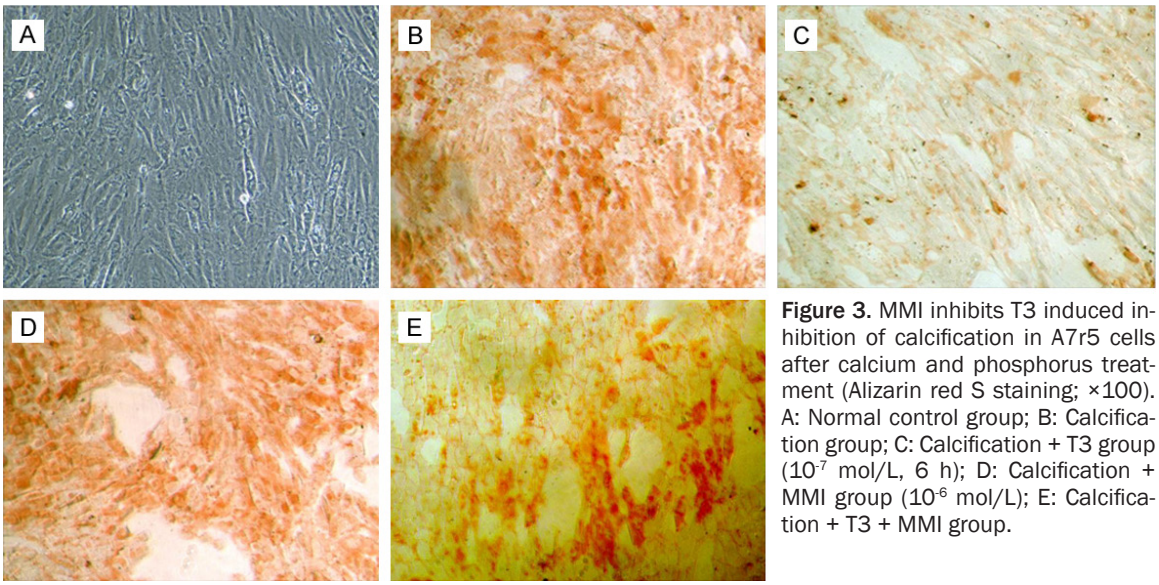

Figure 3. MMI inhibits T3 induced inhibition of calcification in A7r5 cells after calcium and phosphorus treatment (Alizarin red S staining; ×100). A: Normal control group; B: Calcification group; C: Calcification + T3 group (10^{-7} mol/L, 6 h); D: Calcification + MMI group (10^{-6} mol/L); E: Calcification + T3 + MMI group.

Effects of T3 on the osteocalcin content and ALP activity of calcium and phosphorus treated A7r5 cells

The BGP content and ALP activity increased significantly in calcified cells. After treatment with T3 at different concentration, the BGP content and ALP activity reduced markedly, and the inhibition was the most evident in Ca+ T3 (10^{-7} mol/L) group. However, this inhibition did not further become more obvious over time, which was ascribed to the low adherence of calcified cells. These findings were consistent with those observed after Alizarin red S staining (**Figure 2**).

Effects of MMI on the T3 induced inhibition of calcification in A7r5 cells after calcium and phosphorus treatment

When compared with normal control group, the orange calcified nodules increased significantly after calcification induction, accompanied by significant increases in BGP content and ALP activity ($P<0.01$). After treatment with 10^{-7} mol/L T3 for 6 h, the number of calcified nodules reduced significantly, and BGP content and ALP activity decreased markedly when compared with calcification group ($P<0.01$). When compared with T3 group, the number of orange calcified nodules increased markedly, and BGP content and ALP activity elevated dramatically in MMI + T3 group ($P<0.01$). These indicate that MMI may antagonize the effects of T3. However, the BGP content and ALP activity in MMI + T3 group were still higher than in calcification group, suggesting that MMI partially antagonizes the effects of T3 (**Figures 3** and **4**).

Effects of T3 on phenotype markers of A7r5 cells after calcium and phosphorus treatment

When compared with normal control group, the mRNA expression of Osterix and Runx2 (two phenotype specific marker) increased signifi-

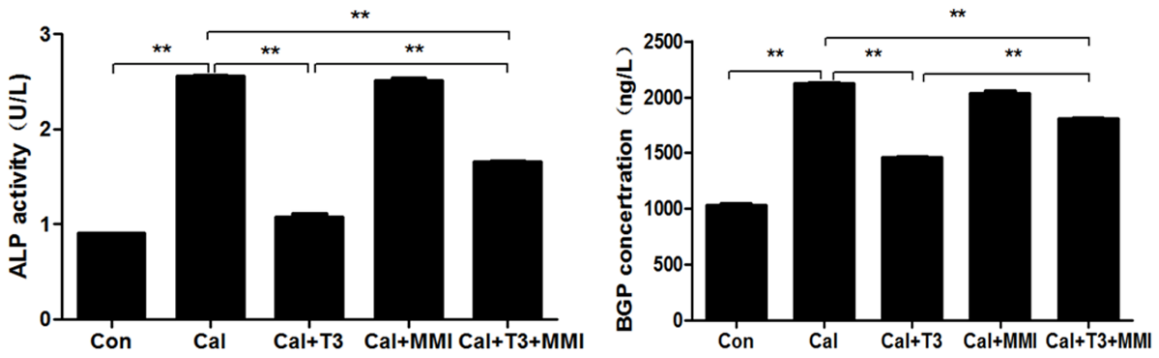

Figure 4. Effects of MMI on the T3 induced inhibition of BGP content and ALP activity in A7r5 cells after calcium and phosphorus treatment. Note: Con: normal control group; Cal: calcification group; Cal + T3: calcification + T3 group (10^{-7} mol/L, 6 h); Cal + MMI: calcification + MMI group (10^{-6} mol/L); Cal + T3 + MMI: calcification + T3 + MMI group. ***P*<0.05.

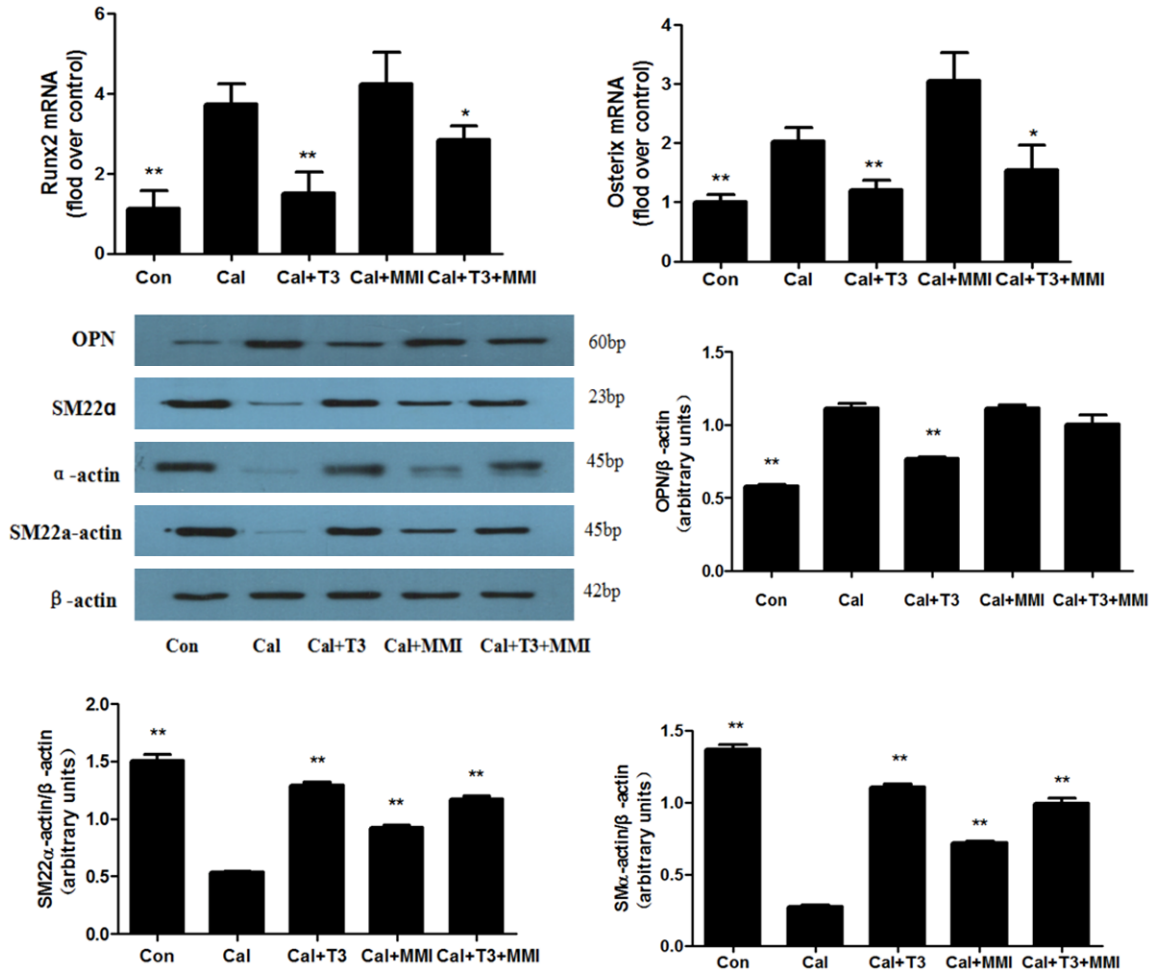

Figure 5. Osterix and Runx2 mRNA expression as well as OPN, SMα and SM22α protein expression in calcium and phosphorus treated A7r5 cells after T3 treatment. Note: Con: normal control group; Cal: calcification group; Cal + T3: calcification + T3 group (10^{-7} mol/L, 6 h); Cal + MMI: calcification + MMI group (10^{-6} mol/L); Cal + T3 + MMI: calcification + T3 + MMI group. **P*<0.05, ***P*<0.01 vs calcification group.

cantly in calcification (P<0.01), the protein expression of OPN (a marker of osteogenesis) elevated markedly (P<0.01), but the protein expression of SMα and SM22α (two markers of contractile phenotype) reduced dramatically (P<0.01) (**Figure 5**).

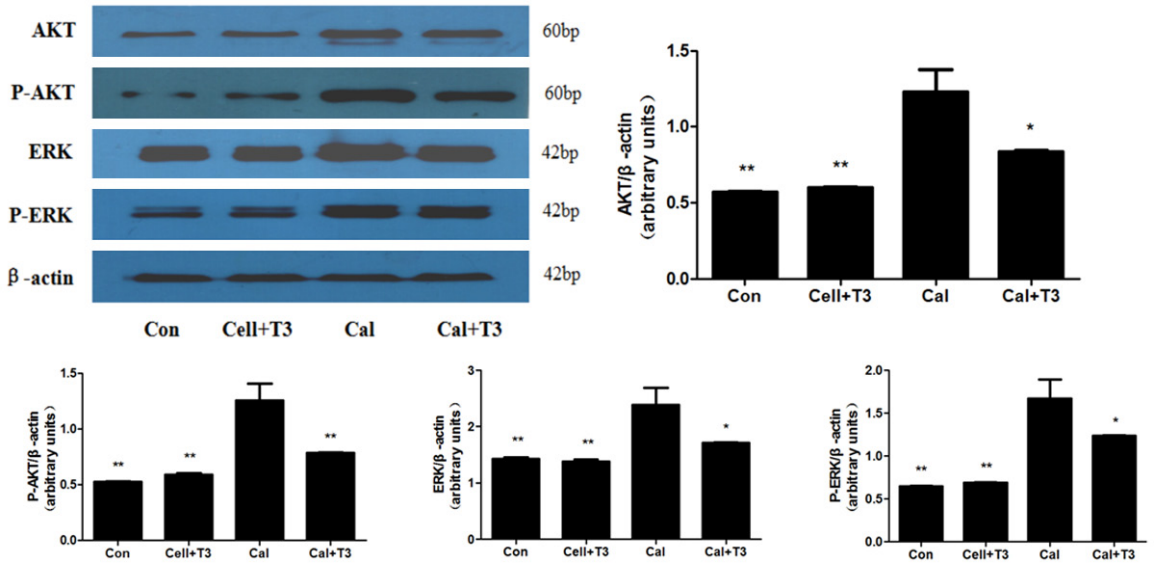

Figure 6. Effects of T3 on the expression of proteins related to phenotype switch in calcium and phosphorus treated A7r5 cells. Note: Con: normal control group; Cell + T3: normal cells + T3 (10^{-7} mol/L, 6 h); Cal: calcification group; Cal + T3: calcification + T3 (10^{-7} mol/L, 6 h); $^{**}P<0.05$, $^{**}P<0.01$ vs calcification group.

When compared with calcification group, the mRNA expression of Osterix and Runx2 reduced significantly in T3 group (P<0.01), accompanied by marked reduction in OPN protein expression (P<0.01) and increase in the protein expression of SMα and SM22α (P<0.01). The mRNA expression of Osterix and Runx2 reduced significantly, the protein expression of SMα and SM22α increased markedly, but OPN protein expression remained unchanged in T3 + MMI group when compared with calcification group (*P*<0.05). These findings were consistent with above finding that MMI partially antagonizes the effects of T3. In addition, MMI alone failed to significantly alter the expression of above molecules (**Figure 5**).

Effects of PD98059 and/or LY294002 on phenotype markers in calcium and phosphorus treated A7r5 cells

When compared with normal control group, the protein expression of ERK1/2, p-ERK, Akt and p-Akt increased significantly (P<0.01) in calcification group. When compared with calcification group, the protein expression of these molecules reduced markedly after T3 treatment (P<0.05), and the reduction in p-Akt protein expression was the most obvious (P<0.01). This suggests that the phenotype switch of calcium and phosphorus induced A7r5 cells is related to the activation of αvβ3/ERK and PI3K/Akt pathways (**Figure 6**).

The αvβ3/ERK blocker PD98059 and/or PI3K/Akt inhibitor LY294002 was used to treat A7r5 cells. Results showed, when compared with calcification group, the mRNA expression of Osterix and Runx2 reduced, and significant difference was observed in Runx2 expression (P<0.01) after inhibitor treatment. In addition, with the increase in inhibitor concentration, OPN protein expression reduced gradually, and protein expression of SMα and SM22α restored progressively. The optimal concentration was 40 mg/L for PD98059 and 30 μmol/L for LY294002. After treatment with inhibitors at optimal concentration, the calcification was still inhibited although calcification induction and T3 treatment were also administered, but the effects were similar to those after treatment with inhibitors alone. This suggests that T3 induced calcification inhibition is not overlapped with that of PD98059 and LY294002. Moreover, the inhibitory effects of LY294002 were more obvious than those of PD98059 (P<0.01), suggesting that calcium and phosphorus induced calcification of A7r5 cells is more related to the activation of PI3K/Akt signaling pathway (**Figure 7**).

Discussion

About 20% of T3 is directly synthesized and secreted by the thyroid, and about 80% of T3 is produced in the liver by the deiodination of T4. T3 is an active form of THs in human body. In

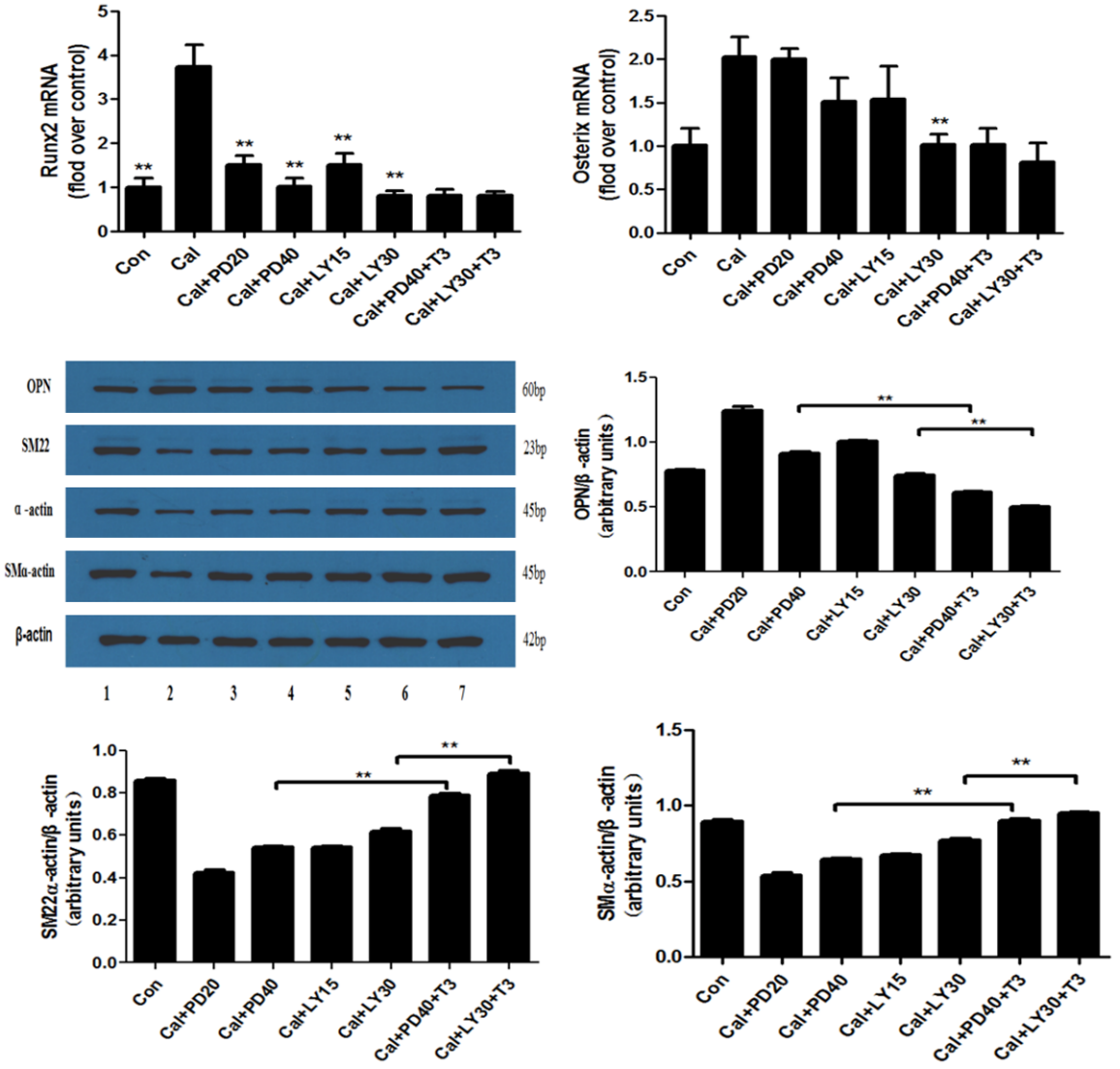

Figure 7. Effects of inhibitors on mRNA expression of Osterix and Runx2 as well as protein expression of OPN, SMα and SM22α in calcium and phosphorus treated A7r5 cells (RT-PCR; Western blotting). 1: Normal control; 2: Calcification + PD98059 (20 mg/L); 3: Calcification + PD98059 (40 mg/L); 4: Calcification + LY294002 (15 μmol/L); 5: Calcification + LY294002 (30 μmol/L); 6: Calcification + PD98059 (40 mg/L) + T3 (6 h, 10^{-7} mol/L); 7: Calcification + LY294002 (30 μmol/L) + T3 (6 h, 10^{-7} mol/L). $^{**}P<0.01$.

non-thyroid systemic diseases (such as chronic liver diseases, kidney diseases, coronary heart disease, infection, malignancy and trauma) and other critical illnesses in neonates such as sepsis, hypoxia and refractory pulmonary hypertension [11-13], low T3 syndrome is often found, which is characterized by subclinical hypothyroidism, low T3, normal T4 and normal TSH. Low T3 syndrome is closely related to the intimal calcification of the carotid artery in chronic kidney disease patients without dialysis and has been an independent risk factor of atherosclerosis [14, 15]. Clinical and subclinical hypothyroidism is a risk factor of atherosclerosis and cardiovascular diseases. FT3 may affect the progression of coronary atherosclerosis [16]. Several studies have shown that T3 is not only a hormone involved in bone metabolism, but may serve as an endogenous protective molecule to inhibit vascular calcification. In our previous studies, results showed T3 was able to inhibit vascular calcification in animals, but the specific mechanism and molecular target are still poorly understood. In the present study, cell calcification model was established to further investigate the molecular mechanism

underlying the T3 induced inhibition of phenotype switching of VSMCs after calcium and phosphorus treatment.

The switch from contractile phenotype to synthetic phenotype in VSMCs is a major process in the vascular calcification under different pathophysiological conditions [17]. This process is reversible and characterized by the presence of matrix vesicles, intracellular calcium overload, increase in ALP activity, calcium deposition in extracellular matrix, increased expression of osteogenesis related proteins such as OPN, up-regulated expression of proteins related to phenotype switch such as Runx2 and Osterix and reduced expression of proteins related to contractile phenotype of VSMCs such as SMα and SM22α [18-20]. In this study, BGP content and OPN protein expression were detected to reflect the calcium and phosphorus induced phenotype switch after T3 treatment. Results showed the BGP content and OPN protein expression reduced significantly after T3 treatment in a concentration dependent manner: the higher the T3 concentration, the lower the BGP content and OPN expression were. This suggests that T3 is able to inhibit the phenotype switch of calcified VSMCs. However, MMI partially antagonized the effects of T3. To further explore whether T3 is directly related to the phenotype switch of VSMCs, the mRNA expression of Runx2 and Osterix (two molecules related to phenotype switch of VSMCs) and protein expression of SMα and SM22α-actin (two markers of contractile phenotype of VSMCs) were detected in A7r5 cells. Results showed, when compared with calcification group, Runx2 and Osterix mRNA expression reduced after T3 treatment and the protein expression of SMα and SM22α-actin restored. This suggests that T3 may inhibit the phenotype switch to inhibit vascular calcification.

αVβ3 is a membrane receptor that can initiate the non-genomic effects of THs [21]. VSMCs may migrate through the subintima, proliferate and secrete a lot of extracellular matrix (ECM) after phenotype switch [22]. ECM (such as OPN) has the characteristic RGD sequence and can bind to β3 subunit of integrin to form focal adhesion complex which then recruits other signaling molecules such as ERK1/2, mediating the biological behaviors (such as proliferation, differentiation, migration, adhesion and apoptosis) of VSMCs [23, 24]. In addition, studies have confirmed that sodium selenite may inhibit the oxidative stress induced vascular calcification [25] in which PI3K/AKT and ERK pathways are activated to regulate the osteogenic differentiation of VSMCs. Thus, in the present study, exogenous T3 and inhibitors were added, and the phosphorylated ERK1/2, PI3K/AKT and other molecules were detected, aiming to investigate the phenotype switch related signaling pathways that can be inhibited by T3 in VSMCs.

Our results showed the ERK1/2, p-ERK, Akt and p-Akt protein expression increased in calcification group, suggesting that calcium and phosphorus induced phenotype switch in A7r5 cells is related to the activation of αvβ3/ERK and PI3K/Akt pathways. In addition, αvβ3/ERK specific inhibitor (PD98059) and/or PI3K/Akt inhibitor (LY294002) [26, 27] were added to the calcification induction medium. Results showed mRNA expression of Osterix and Runx2 reduced after addition of inhibitors, and OPN protein expression reduced and protein expression of SMα and SM22α restored gradually with the increase in inhibitor concentration. To further investigate the specific signaling pathway involved in T3 induced inhibition of phenotype switch in calcium and phosphorus treated VSMCs, inhibitors at optimal concentrations and T3 were added to the calcification induction medium, and then the expression of proteins and transcription factors related to phenotype switch was detected. Results showed LY294002 had a better inhibitor effect as compared to PD98059, which further confirms that T3 induced inhibition of phenotype switch of VSMCs is more closely related to PI3K/Akt signaling pathway.

Taken together, cell calcification model is successfully established by treatment of rat A7r5 cells with calcium and phosphorus and our results indicate that the calcification related phenotype switch is related to the activation of αvβ3/ERK and PI3K/Akt pathways. At molecule level, we further confirm that T3 mainly activates PI3K/Akt signaling pathway to inhibit the calcium and phosphorus induced phenotype switch of VSMCs. These findings suggest that T3 is an important endogenous protective hormone that can inhibit vascular calcification and inhibit the osteogenic phenotype of VSMCs. Our findings provide theoretical evidence for

the molecular mechanism underlying the T3 induced inhibition of phenotype switch in VSMCs and the clinical reversal of vascular remodeling.

Acknowledgements

This study was supported by the National Natural Science Foundation of China (No. 81370972 to BH. Zhang).

Disclosure of conflict of interest

None.

Address correspondence to: Zhichun Feng, Department of Neonatology, Affiliated Bayi Children's Hospital, Clinical Medical College in PLA Army General Hospital, Southern Medical University, Beijing 100007, China. E-mail: drfengzc@fmmu.edu.cn; Baohong Zhang, Department of Pediatrics, The Hospital of Tsinghua University, Beijing 100084, China. E-mail: hongbaozhang@mail.tsinghua.edu.cn

References

[1] Jeziorska M, McCollum C and Wooley DE. Observations on bone formation and remodelling in advanced atherosclerotic lesions of human carotid arteries. Virchows Arch 1998; 433: 559-565.

[2] Kurabayashi M. [Vascular Calcification - Pathological Mechanism and Clinical Application. Role of vascular smooth muscle cells in vascular calcification]. Clin Calcium 2015; 25: 661-669.

[3] Pei C, Qin S, Wang M and Zhang S. Regulatory mechanism of human vascular smooth muscle cell phenotypic transformation induced by NELIN. Mol Med Rep 2015; 12: 7310-7316.

[4] Chen JJ, Zhang J, Cai Y, Zhou YB, Wen GB, Tang CS, Qi YF and Jiang ZS. C-type natriuretic peptide inhibiting vascular calcification might involve decreasing bone morphogenic protein 2 and osteopontin levels. Mol Cell Biochem 2014; 392: 65-76.

[5] Herencia C, Rodriguez-Ortiz ME, Munoz-Castaneda JR, Martinez-Moreno JM, Canalejo R, Montes de Oca A, Diaz-Tocados JM, Peralbo-Santaella E, Marin C, Canalejo A, Rodriguez M and Almaden Y. Angiotensin II prevents calcification in vascular smooth muscle cells by enhancing magnesium influx. Eur J Clin Invest 2015; 45: 1129-1144.

[6] Gao J, Zhang K, Chen J, Wang MH, Wang J, Liu P and Huang H. Roles of aldosterone in vascular calcification: An update. Eur J Pharmacol 2016; 786: 186-193.

[7] Balli M, Cetin M, Tasolar H, Uysal OK, Yilmaz M, Durukan M, Elbasan Z and Cayli M. The relationship between serum thyroid hormone levels, subclinical hypothyroidism, and coronary collateral circulation in patients with stable coronary artery disease. Turk Kardiyol Dern Ars 2016; 44: 130-136.

[8] Lee S and Farwell AP. Euthyroid Sick Syndrome. Compr Physiol 2016; 6: 1071-1080.

[9] de Vries EM, Fliers E and Boelen A. The molecular basis of the non-thyroidal illness syndrome. J Endocrinol 2015; 225: R67-81.

[10] Zhang J, Chang JR, Duan XH, Yu YR and Zhang BH. Thyroid hormone attenuates vascular calcification induced by vitamin D3 plus nicotine in rats. Calcif Tissue Int 2015; 96: 80-87.

[11] Mancini A, Di Segni C, Raimondo S, Olivieri G, Silvestrini A, Meucci E and Curro D. Thyroid Hormones, Oxidative Stress, and Inflammation. Mediators Inflamm 2016; 2016: 6757154.

[12] da Silva MH, de Araujo MC, Diniz EM, Ceccon ME and de Carvalho WB. Nonthyroidal illnesses syndrome in full-term newborns with sepsis. Arch Endocrinol Metab 2015; 59: 528-534.

[13] Vakilian F, Attaran D, Shegofte M, Lari S and Ghare S. Assessment of Thyroid Function in Idiopathic Pulmonary Hypertension. Res Cardiovasc Med 2016; 5: e29361.

[14] Fan J, Yan P, Wang Y, Shen B, Ding F and Liu Y. Prevalence and Clinical Significance of Low T3 Syndrome in Non-Dialysis Patients with Chronic Kidney Disease. Med Sci Monit 2016; 22: 1171-1179.

[15] Afsar B, Yilmaz MI, Siriopol D, Unal HU, Saglam M, Karaman M, Gezer M, Sonmez A, Eyileten T, Aydin I, Hamcan S, Oguz Y, Covic A and Kanbay M. Thyroid function and cardiovascular events in chronic kidney disease patients. J Nephrol 2016; [Epub ahead of print].

[16] Zhang Y, Kim BK, Chang Y, Ryu S, Cho J, Lee WY, Rhee EJ, Kwon MJ, Rampal S, Zhao D, Pastor-Barriuso R, Lima JA, Shin H and Guallar E. Thyroid hormones and coronary artery calcification in euthyroid men and women. Arterioscler Thromb Vasc Biol 2014; 34: 2128-2134.

[17] Yoshiyama S, Chen Z, Okagaki T, Kohama K, Nasu-Kawaharada R, Izumi T, Ohshima N, Nagai T and Nakamura A. Nicotine exposure alters human vascular smooth muscle cell phenotype from a contractile to a synthetic type. Atherosclerosis 2014; 237: 464-470.

[18] Lee SJ, Baek SE, Jang MA and Kim CD. Osteopontin plays a key role in vascular smooth muscle cell proliferation via EGFR-mediated activation of AP-1 and C/EBPbeta pathways. Pharmacol Res 2016; 108: 1-8.

[19] Xie XL, Nie X, Wu J, Zhang F, Zhao LL, Lin YL, Yin YJ, Liu H, Shu YN, Miao SB, Li H, Chen P

and Han M. Smooth muscle 22alpha facilitates angiotensin II-induced signaling and vascular contraction. J Mol Med (Berl) 2015; 93: 547-558.
[20] Lei Y, Sinha A, Nosoudi N, Grover A and Vyavahare N. Hydroxyapatite and calcified elastin induce osteoblast-like differentiation in rat aortic smooth muscle cells. Exp Cell Res 2014; 323: 198-208.
[21] Davis PJ, Sudha T, Lin HY and Mousa SA. Thyroid Hormone, Hormone Analogs, and Angiogenesis. Compr Physiol 2015; 6: 353-362.
[22] Amin M, Pushpakumar S, Muradashvili N, Kundu S, Tyagi SC and Sen U. Regulation and involvement of matrix metalloproteinases in vascular diseases. Front Biosci (Landmark Ed) 2016; 21: 89-118.
[23] Chaterji S, Lam CH, Ho DS, Proske DC and Baker AB. Syndecan-1 regulates vascular smooth muscle cell phenotype. PLoS One 2014; 9: e89824.
[24] Jeong JY, Son Y, Kim BY, Eo SK, Rhim BY and Kim K. Multiple Signaling Pathways Contribute to the Thrombin-induced Secretory Phenotype in Vascular Smooth Muscle Cells. Korean J Physiol Pharmacol 2015; 19: 549-555.
[25] Liu H, Li X, Qin F and Huang K. Selenium suppresses oxidative-stress-enhanced vascular smooth muscle cell calcification by inhibiting the activation of the PI3K/AKT and ERK signaling pathways and endoplasmic reticulum stress. J Biol Inorg Chem 2014; 19: 375-388.
[26] Huang J, Huang H, Wu M, Li J, Xie H, Zhou H, Liao E and Peng Y. Connective tissue growth factor induces osteogenic differentiation of vascular smooth muscle cells through ERK signaling. Int J Mol Med 2013; 32: 423-429.
[27] Liu QF, Yu HW, Sun LL, You L, Tao GZ and Qu BZ. Apelin-13 upregulates Egr-1 expression in rat vascular smooth muscle cells through the PI3K/Akt and PKC signaling pathways. Biochem Biophys Res Commun 2015; 468: 617-621.